J Mater Sci: Mater Electron (2023) 34:487

Color tuneability behaviour and energy transfer analysis on Dy^{3+}-Eu^{3+} co-doped glasses for NUV-WLEDs application

M. Monisha[1], M. I. Sayyed[2,3], Nirmal Mazumder[4], Jack Arayro[5], and Sudha D. Kamath[1,*]

[1] *Department of Physics, Manipal Institute of Technology, Manipal Academy of Higher Education, Manipal 576 104, Karnataka, India*
[2] *Department of Physics, Faculty of Science, Isra University, Amman, Jordan*
[3] *Department of Nuclear Medicine Research, Institute for Research and Medical Consultations (IRMC), Imam Abdulrahman bin Faisal University (IAU), P.O. Box 1982, Dammam 31441, Saudi Arabia*
[4] *Department of Biophysics, Manipal School of Life Sciences, Manipal Academy of Higher Education, Manipal 576 104, Karnataka, India*
[5] *College of Engineering and Technology, American University of the Middle East, Egaila, Kuwait*

Received: 7 October 2022
Accepted: 24 November 2022
Published online: 11 February 2023

ABSTRACT

A series of Dy^{3+} and Eu^{3+} co-doped zinc aluminoborosilicate (ZABS) glasses were synthesized by a high-temperature melt-quenching method. Visible and NIR transitions of Dy^{3+}-Eu^{3+} ions are observed through absorption spectra. A reverse trend in the optical band gap values and Urbach energy are seen with addition of Eu^{3+} ions. Photoluminescence studies recorded under different excitation wavelengths showed a variation in the emission intensities and prevailed the color tuneability behaviour of dopants. The energy transfer between Dy^{3+} and Eu^{3+} ions are studied through emission profiles, energy level diagram, and decay curves. The type of multipolar interaction between Dy^{3+} and Eu^{3+} are understood via Inokuti-Hirayama (IH) model and Dexter energy model. The CIE chromaticity coordinates, and correlated color temperature (CCT) values suggest that the prepared glasses can be used for light emitting diode application when excited at near-ultraviolet region.

1 Introduction

White light emission from single light emitting components like phosphor played a significant role in the lighting industry due to its peculiar property of giving high brightness and color quality [1]. An attempt to obtain white light with tri-color-based phosphors fascinated researchers in recent times [2]. However, such a method resulted a variation in the color of phosphors as time goes on and needs dif-

Address correspondence to E-mail: sudhakamath6@gmail.com

ferent drive voltages for different color emitting components [3]. Therefore, in an urge to gain white light from an identical luminescent center *via* the combination of different color emissions, different methods were attempted. One of the most pivotal methods to obtain a single-phased white light with uplifted emission is through energy transfer between two rare earths i.e., a sensitizer and an activator such as Tb^{3+}/Dy^{3+}, Ce^{3+}/Dy^{3+} [4, 5]. In common, Dy^{3+} ions are included as sensitizer in co-doped materials due to their intense emission bands in the blue (482 nm) and yellow (575 nm) regions corresponding to the transition levels of $^4F_{9/2} \rightarrow {}^6H_{15/2}$ and $^4F_{9/2} \rightarrow {}^6H_{15/2}$ [6]. Nevertheless, the lack of red-component in Dy^{3+} makes it unsuitable for practical applications [7]. Hence, an efficient red light emitting material should be combined with Dy^{3+} to give a stable white light. Among the lanthanides, Eu^{3+} is known to emit intense red light from the $^5D_0 \rightarrow {}^7F_1$ and $^5D_0 \rightarrow {}^7F_2$ levels falling in the visible region such as 590 nm and 613 nm [8]. Combining Dy^{3+} with Eu^{3+} will tend to enforce the europium emission, and thereby rectify the lack of red-component with singly doped Dy^{3+} ions. The yellow to blue emission intensity ratio (Y/B ratio) in Dy^{3+}based materials can be tuned with incorporation of Eu^{3+} ions in smaller intervals. When Dy^{3+} combined with Eu^{3+} materials are excited with n-UV light source the Dy^{3+} ions absorb the incident light, and they transfer the part of absorbed energy non-radiatively to Eu^{3+} ions causing emissions. Moreover, the white light obtained via co-doping can be adjusted or tuned from a cold white light to warm white light with increasing the Eu^{3+}content [9]. Therefore, Dy^{3+} and Eu^{3+} co-doped materials have gained lots of interest in the past years.

Compared to rare earth doped phosphors [7, 8], glasses act as an efficient center due to their strong dispersion of RE (rare earth) ions in the glass matrix, better thermal stability, and sharp electronic spectra of RE ions with less crystal-field splitting. Many research articles reported the color tuneability, and energy transfer of Dy^{3+} and Eu^{3+} co-doped glasses with different glass matrices [11–17]. Among different host matrices, borosilicate glasses with two major component such as B_2O_3 and SiO_2 are a potential choice since they own several exceptional properties like high thermal resistance, easy solubility of RE ions, good mechanical properties, and low thermal expansion coefficient [10]. Therefore, in the present work the color tuneability behaviour of co-doped zinc alumino borosilicate glasses, with varying Eu^{3+} concentrations, under different excitation wavelengths is analyzed. Also, the type of energy transfer interaction from the sensitizer (Dy^{3+}) to the activator (Eu^{3+}) are reported using Inokuti-Hirayama (IH) fitting and Dexter energy transfer model. The obtained results showed the suitability of prepared glasses for near-ultraviolet W-LEDs applications.

2 Experimental details

Transparent glasses with glass matrix formula given as $20SiO_2–(20–x–y)B_2O_3–10Al_2O_3–10ZnO–30NaF–10ZnF_2–xDy_2O_3–yEu_2O_3$ (where x = 0.5 mol% and y = 0, 0.1, 0.5, 1.0, 1.5, 2.0 and 2.5 mol%) were synthesized using high-temperature melt-quenching method. The starting materials were initially taken by proper weighing of them to get a total of 10-gram quantity of glass. After a constant grinding of raw materials, they are melted in an alumina crucible at 1320 °C for 2 h. The formed melt is cascaded quickly on a pre-heated brass plate at 350 °C. Once the melt is released or quenched on the brass plate, it immediately forms a solid glass. The solid glass is further annealed for 2 h at the quenched temperature to reduce thermal stresses, avoid breaking of glass and to maintain transparency. The glasses were polished to get a smooth surface and their thicknesses was reduced to ~ 2 mm for optical studies. The prepared glasses were labelled as ZABSDE0, ZABSDE1, ZABSDE2, ZABSDE3, ZABSDE4, ZABSDE5 and ZABSDE6, respectively.

3 Result and discussion

3.1 UV-Visible-NIR studies

The absorption spectra recorded for the synthesized glasses showed several peaks comprising of both Dy^{3+} and Eu^{3+} ions. In the case of Dy^{3+}, the absorbance excitation occurs from a single ground state at $^6H_{15/2}$ while for Eu^{3+} there are two ground states of $^7F_0$ and $^7F_1$ such that the absorption transitions occur from both these levels. Figure 1(a) shows the UV-Visible part of the absorption spectra. Here the transitions peaks corresponding to Dy^{3+} ions are located at 350 ($^6P_{7/2}$), 364 ($^4I_{11/2} + {}^6P_{5/2}$), 387 ($^4I_{13/2} + {}^4F_{7/2}$), 425 ($^4G_{11/2}$), 452 ($^4I_{15/2}$), and 473 nm ($^4F_{9/2}$); whereas

the transitions peaks of Eu^{3+} ions are observed at 362 ($^7F_0 \rightarrow {}^5D_4$), 376 ($^7F_0 \rightarrow {}^5L_7$), 383 ($^7F_0 \rightarrow {}^5G_2$), 393 ($^7F_0 \rightarrow {}^5L_6$), 414 ($^7F_0 \rightarrow {}^5D_3$), 464 ($^7F_0 \rightarrow {}^5D_2$), 525 ($^7F_0 \rightarrow {}^5D_1$), and 532 nm ($^7F_1 \rightarrow {}^5D_1$). The absorption intensity of the peaks is improved with co-doping of Eu^{3+} ions to Dy^{3+} ions [11, 12]. The Dy^{3+} peaks are seen for all co-doped (Dy^{3+}-Eu^{3+}) glasses except for the peaks present around 376 nm, 393 nm, 414 nm, 525 nm, and 532 nm which are purely due to Eu^{3+} ions [12]. For Dy^{3+} singly doped glass, the peaks observed at 364 and 387 nm gets slightly shifted to the lower wavelength side on addition of Eu^{3+} ions for co-doped glasses. Thus, the overlapping of energy levels of Dy and Eu in the ultraviolet region exist and are shown in yellow colour in the inset of Fig. 1. This overlapping of Dy^{3+} and Eu^{3+} energy levels signifies some sort of energy transfer behaviour existing in the glasses. In NIR region lying between 700 and 2500 nm (Fig. 1b), the Dy^{3+} ions transitions are seen at 752 ($^6F_{3/2}$), 801 ($^6F_{5/2}$), 899 ($^6F_{7/2} + {}^6H_{5/2}$), 1087 ($^6F_{9/2} + {}^6H_{7/2}$), 1267 ($^6F_{11/2} + {}^6H_{9/2}$), and 1687 nm ($^6H_{11/2}$) and the Eu^{3+} transitions are seen at 2090 nm ($^7F_0 \rightarrow {}^7F_6$) and 2203 nm ($^7F_1 \rightarrow {}^5F_6$). Increasing Eu^{3+} concertation in the glass also improves the absorbance intensity of Dy^{3+} and Eu^{3+} ions [16, 17].

Figure 2a represents the absorption band-edge plot which shows a red shift in the band-edges of the glasses with varying Eu^{3+} concentration. The optical band gap of the glasses was determined by drawing Tauc's plot (Fig. 2b) using the following relation given as [18, 19].

$$(\alpha - hv)^{1/n} = B(hv - E_g) \quad (1)$$

In the Eq. (1), the terms α, h, v, E_g denote the absorption coefficient, Planck's constant, photon frequency, and bandgap energy. The term B is a constant known as band-tailing parameter and n is the power factor that determines the nature of the electronic transition. A value of $n = \frac{1}{2}$ shows a direct bandgap and while $n = 2$ indicates an indirect one. For amorphous and disordered materials such as glasses, n takes up the value as 2 because of the indirect transitions of rare earth ions. The band gap values are given in Table 1. The exponential tail seen at the absorption edge of the glasses indicates that there may be some sort of defect states or disorderness present which are created due to the incident high energy ultra-violet radiation and heavy element doping such as Dy, Eu. The exponential tail is otherwise called Urbach tail, and it determines the number of defects or disorderness present in the glasses. The defects are quantified in terms of Urbach energy (eV) which can be obtained by plotting ln (α) against hv (photon energy), and then taking the inverse of the slope value obtained [20] as shown for ZABSDE1 glass in Fig. 3. These values are presented in Table 1. The reverse trend in bandgap energy and Urbach energy values suggest that, the more the localized energy levels/defects in the glass system, the less the bandgap energy becomes. Thus, the glasses with higher bandgap values show lower Urbach energy values.

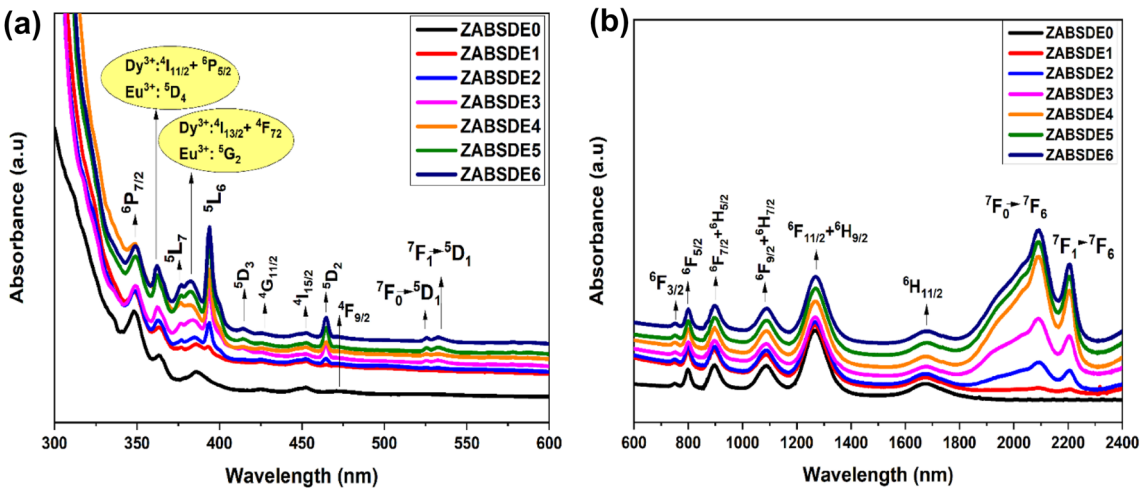

Fig. 1 **a** UV-Visible and **b** NIR absorption spectra recorded for Dy^{3+}-Eu^{3+} co-doped glasses

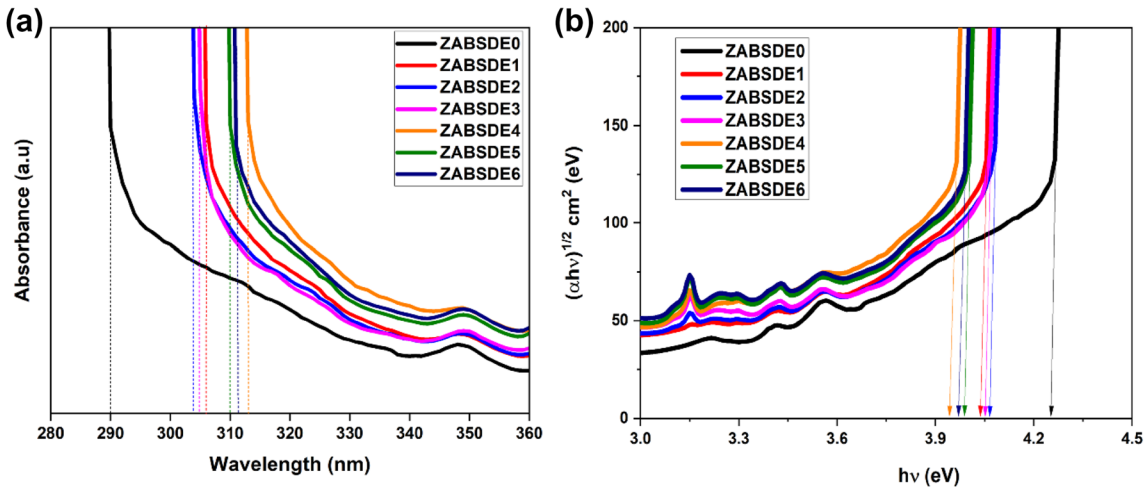

Fig. 2 **a** Absorption band-edge and **b** Tauc's plot illustrating indirect optical band gap

Table 1 Absorption band-edge (nm), indirect optical bandgap (E_g) energy, and Urbach energy (E_U) for Dy^{3+}-Eu^{3+} co-doped ZABS glasses

Glass Code	Absorption band-edge (nm)	Indirect Optical bandgap energy (eV)	Urbach energy (eV)
ZABSDE0	290	4.27	0.3802
ZABSDE1	306	4.03	0.4101
ZABSDE2	303	4.06	0.3949
ZABSDE3	305	4.05	0.3983
ZABSDE4	313	3.94	0.4612
ZABSDE5	310	3.98	0.4114
ZABSDE6	311	3.97	0.4299

3.2 Photoluminescence measurements

3.2.1 *Excitation and emission studies*

The excitation spectra for the co-doped glasses were recorded at 575 and 613 nm wavelengths and are given in Fig. 4a, b, respectively. Under 575 nm, both Dy^{3+} singly doped glass and Dy^{3+}/Eu^{3+} co-doped glasses showed Dy^{3+} peaks at 325 ($^4M_{17/2}$+$^6P_{3/2}$), 350 ($^6P_{7/2}$), 364 ($^4I_{11/2}$+$^6P_{5/2}$), 387 ($^4I_{13/2}$+$^4F_{7/2}$), 425 ($^4G_{11/2}$), 453 ($^4I_{15/2}$), and 473 nm ($^4F_{9/2}$) from $^6H_{15/2}$ ground level [20]. But the Eu^{3+} ions do not promote any kind of transitions with 575 nm. Moreover, the intensity of the observed peaks decreases on co-doping with Eu^{3+} ions. At 2.5 mol% of Eu^{3+} dopant the Dy^{3+} peaks achieved a very low intensity as seen from Fig. 4a. With 613 nm wavelength, the Dy^{3+}

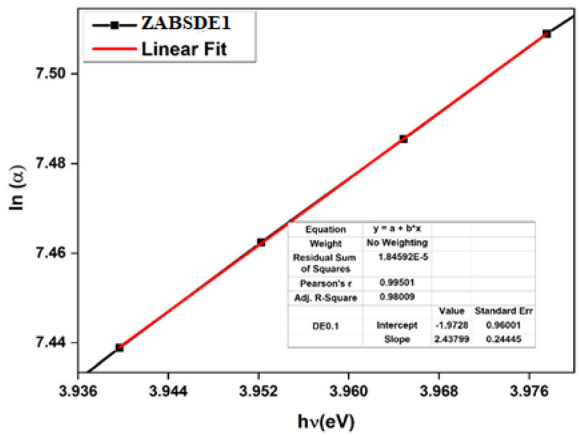

Fig. 3 Urbach energy plot showing the linear fit of *hν* versus *ln(α)* for ZABSDE1 glass

singly doped glass shows very low intensity of Dy^{3+} peaks at 342, 350, 364, 387, 425, and 450 nm given in the inset of Fig. 4b. With addition of Eu^{3+} ions even the low intensity peaks of Dy^{3+} are suppressed

completely and the only peak at 350 nm ($^6P_{7/2}$) is seen with minimum intensity in co-doped glasses. This means that 613 nm is an excitation source for Eu^{3+} ions which only triggers them to get excited to higher energy levels located at 319 ($^7F_0 \rightarrow {}^5H_6$), 362 ($^7F_0 \rightarrow {}^5D_4$), 382 ($^7F_0 \rightarrow {}^5G_2$), 393 ($^7F_0 \rightarrow {}^5L_6$), 414 ($^7F_0 \rightarrow {}^5D_3$), 465 ($^7F_0 \rightarrow {}^5D_2$), 525 ($^7F_0 \rightarrow {}^5D_1$) and 533 nm ($^7F_1 \rightarrow {}^5D_1$) [21].

The emission spectra recorded at λ_{exc} = 350 nm is shown in Fig. 5a. Under 350 nm, the Dy^{3+} singly doped glass features three emission bands from $^4F_{9/2}$ excited level to ground levels lying at 482 ($^6H_{15/2}$), 575 ($^6H_{13/2}$) and 663 nm ($^6H_{11/2}$); whereas the Dy^{3+}-Eu^{3+} co-doped glasses show five emission bands in which Eu^{3+} are located at 613 ($^5D_0 \rightarrow {}^7F_2$) and 701 nm ($^5D_0 \rightarrow {}^7F_4$) along with emissions of Dy^{3+} at 482 nm, 575 and 663 nm. On exciting Dy^{3+} ions the emission bands corresponding to Eu^{3+} are also observed in the spectra. Most importantly, increasing the Eu^{3+} concentration leads to the decrease in Dy^{3+} emission intensity and this assures the possibility energy transfer from Dy^{3+} to Eu^{3+}. On exciting the glasses under 393 nm wavelength (Fig. 5b), the emission spectra show a steady decrease in the Dy^{3+} band at 482 nm whereas the Dy^{3+} peak at 575 nm splits up into two peaks i.e., the original peak at 575 nm (Dy^{3+}) and newly formed peak at 590 nm (Eu^{3+}). This spectral energy level splitting is seen when increasing the concentration of Eu^{3+} ions beyond 0.5 mol% (given in inset of Fig. 5b). The intense emission peak of Eu^{3+} seen at 613 nm ($^5D_0 \rightarrow {}^7F_2$) reaches a maximum height for ZABSDE3 glass i.e., at 1.0 mol% of Eu^{3+} co-doping. Above this concentration, the emission intensity decreased slowly. Hence, the concentration quenching was achieved for Eu^{3+} co-doping beyond 1.0 mol% under 393 nm excitation [16, 17]. This sort of concentration quenching in the co-doped glasses with the excitation source of the activator could be due to the energy transfer between activator ions (i.e., Eu^{3+} ions), possibly due to radiative re-absorption. Thus, ZABSDE3 glass is regarded as the optimum candidate with excitation in the near ultra-violet region (393 nm).

3.2.2 *Spectral overlap and energy level diagram*

Figure 6a depicts the overlap diagram that includes Dy^{3+} emission and Eu^{3+} excitation in singly doped glass. The PL (Photoluminescence spectroscopy) characteristics assure the blue and yellow emissions (Dy^{3+}) as well as deep red emissions (Eu^{3+}) from the glasses. The spectral overlap image reveals that the emission band of Dy^{3+} at 482 nm ($^4F_{9/2} \rightarrow {}^6H_{15/2}$) exhibits an overlap with the excitation band of Eu^{3+} at 464 nm ($^7F_0 \rightarrow {}^5D_2$). This spectral overlap of donor ion's emission spectrum (Dy^{3+}) and acceptor ion's excitation spectrum (Eu^{3+}) indicates a migration occurring between them. Figure 6b shows the energy level diagram for Dy^{3+} and Eu^{3+} transitions. As seen from the excitation spectra, the two emission wavelengths at 575 and 613 nm are used for promoting the Dy^{3+} and Eu^{3+} ions to their upper excited levels. Later both the Dy^{3+} and Eu^{3+} ions reach one of their intermediate levels at $^4F_{9/2}$ and $^5D_0$ through non-radiative relaxation. On reaching the intermediate level at $^4F_{9/2}$, Dy^{3+} ions transfer part of the energy to Eu^{3+}

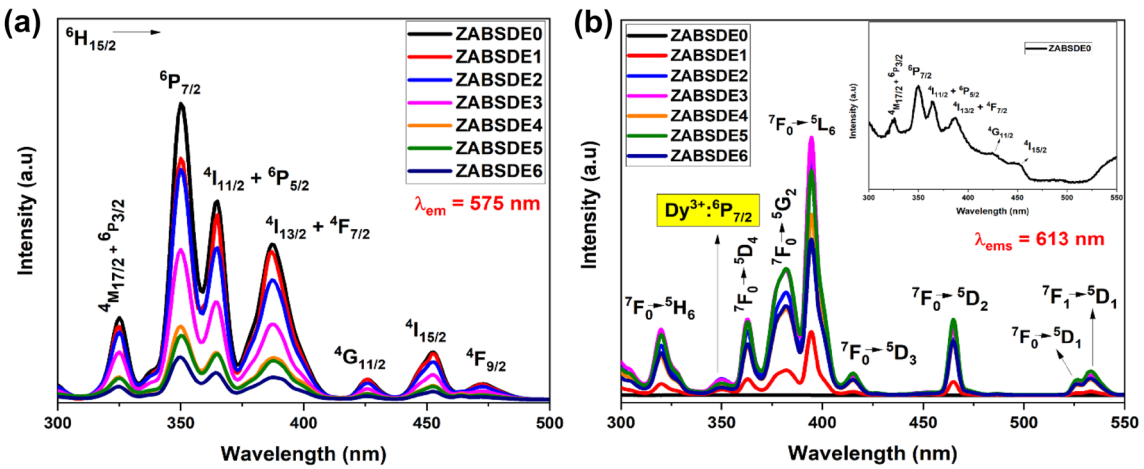

Fig. 4 Excitation spectra of Dy^{3+}-Eu^{3+} co-doped glasses recorded under **a** 575 nm and **b** 613 nm wavelengths

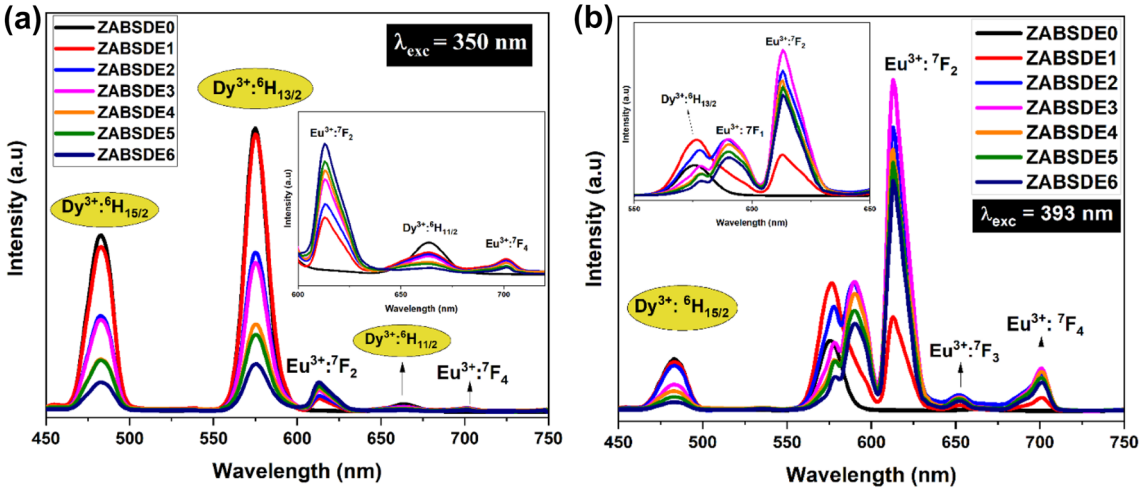

Fig. 5 Emission spectra pertaining to **a** 350 nm excitation wavelength of Dy^{3+} ions and **b** 393 nm excitation wavelength of Eu^{3+} ions

ions lying in the metastable state at $^5D_0$. This is possible because the energy level of Dy^{3+} ($^4F_{9/2}$) is approximately 21,000 cm^{-1} which is slightly greater than the energy levels of Eu^{3+} at $^5D_1$ (19,020 cm^{-1}) and $^5D_0$ ($\sim$ 17,277 cm^{-1}) making the Dy^{3+} ions a resourceful sensitizer for Eu^{3+} ions [16]. The green arrow shown in Fig. 6b denotes the transfer of energy from Dy^{3+} to Eu^{3+}. After the energy transfer process, Dy^{3+} ions reach their ground levels at $^6H_{15/2}$, $^6H_{13/2}$ and $^6H_{11/2}$ by giving visible emissions in blue (482 nm), yellow (575 nm) and red (663 nm) regions, respectively. Similarly, the Eu^{3+} ions absorb the energy from Dy^{3+} and undergo emissions to the lower levels at $^7F_1$ (590 nm), $^7F_2$ (613 nm), $^7F_3$ (652 nm), $^7F_4$ (701 nm).

3.2.3 *Decay analysis of Dy^{3+} -Eu^{3+} co-doped glasses*

The decay profile of the $^4F_{9/2} \rightarrow {}^6H_{15/2}$ transition of Dy^{3+} ions under 350 nm excitation and 575 nm emission is given in Fig. 7a. All the glasses show a bi-exponential behaviour under 350 nm. The lifetime values are drawn out using ExpDec2 Fit as shown in

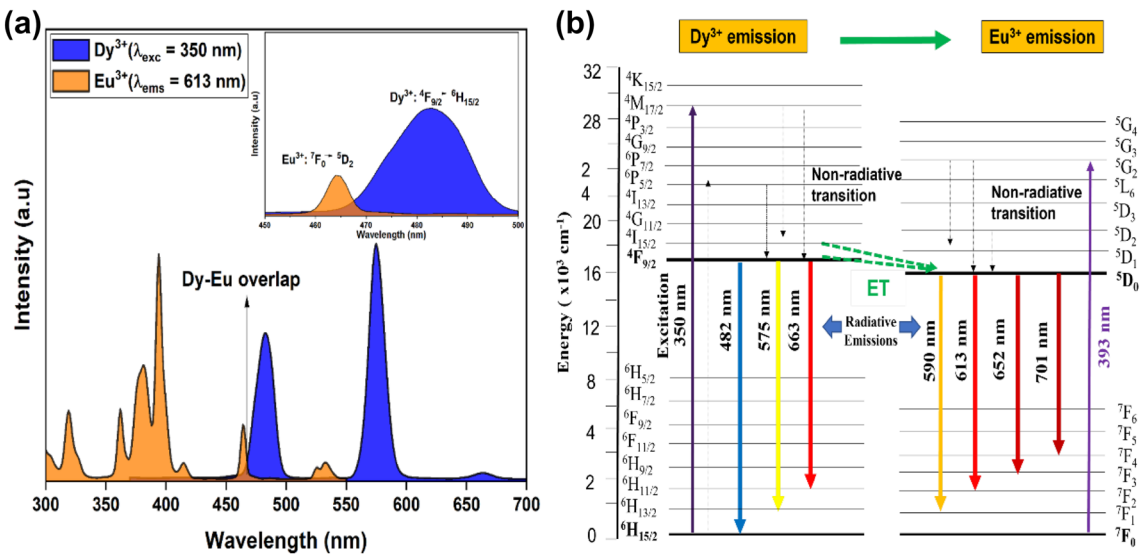

Fig. 6 **a** Overlap diagram of excitation and emission spectra of Dy^{3+} and Eu^{3+} and **b** partial energy level diagram

Fig. 7b. The bi-exponential fitting equation is given as [20].

$$I = A_1 exp\left(\frac{-x}{t_1}\right) + A_2 exp\left(\frac{-x}{t_2}\right), \quad (2)$$

where A_1 and A_2 are the constants, t_1 and t_2 are the luminescence decay times. Using the two lifetime values, the average lifetime is determined via the Eq.

$$\tau_E = \frac{(A_1 t_1^2 + A_2 t_2^2)}{(A_1 t_1 + A_2 t_2)} \quad (3)$$

The calculated lifetime decreases with increasing Eu^{3+} concentrations, and the values are obtained at 512.34 µs, 497.53 µs, 481.64 µs, 470.94 µs, 462.18 µs, 445.53 µs and 433.74 µs corresponding to samples ZABSDE0, ZABSDE1, ZABSDE2, ZABSDE3, ZABSDE4, ZABSDE5, ZABSDE6, respectively. This decrease in lifetime of Dy^{3+} ions in level $^4F_{9/2}$ clearly indicates that energy transfer occurs from Dy^{3+} ions to Eu^{3+} ions [22]. Similarly, the decay study of the $^5D_0 \rightarrow {}^7F_2$ transition of Eu^{3+} ions under 350 nm excitation and 613 nm emission is given in Fig. 8a. The representative fitting plot is given in Fig. 8b. The bi-exponential behaviour is observed in this case also. Here the excitation of Dy^{3+} ions improved the lifetime of $^5D_0$ state of Eu^{3+} ions though energy transfer. The lifetime of the $^5D_0$ level of Eu^{3+} ions record a highest value for 1.0 mol% (ZABSDE3) glass; then the lifetime values are decreased beyond this concentration. The decrease in lifetime is due to the more amount of energy transfer from Dy^{3+} to Eu^{3+} ions possibly beyond 1.0 mol%. The values are given in Table 2. The lifetime values are then used to calculate other parameters such as energy transfer efficiency (η_{ET}), and the probability of energy transfer (P_{ET}) applying the following formulas [23].

$$\eta_{ET} = 1 - \left(\frac{\tau_d}{\tau_{d_o}}\right) \times 100 \quad (4)$$

$$P_{ET} = \frac{1}{\tau_d} - \frac{1}{\tau_{d_o}}, \quad (5)$$

where τ_{d_o} and τ_d are the inherent decay times of donor (Dy) in the presence and absence of acceptor (Eu). The obtained values are listed in Table 2. The increase in energy transfer efficiency is seen from 2 to 15% with increasing the Eu^{3+} ions.

3.2.4 *Inokuti-hirayama fitting*

The luminescence quenching via non-radiative energy transfer from $^4F_{9/2}$ (Dy^{3+}) level to $^5D_0$ (Eu^{3+}) level can be explained by Inokuti-Hirayama (I-H) model. Using the I-H model, it is simpler to identify the nature of energy transfer between the donor and the acceptor. The non-exponential decay curves are fitted to the I-H model which implies the following relation,

$$I = I_O exp\left[-\frac{t}{\tau_o} - Q\left(\frac{t}{\tau_o}\right)^{3/S}\right] \quad (6)$$

Here, S represents the interaction type such that, S = 6, 8, 10 corresponds to dipole-dipole (d-d), dipole-quadrapole (d-q), and quadrapole-quadrapole (q-q)

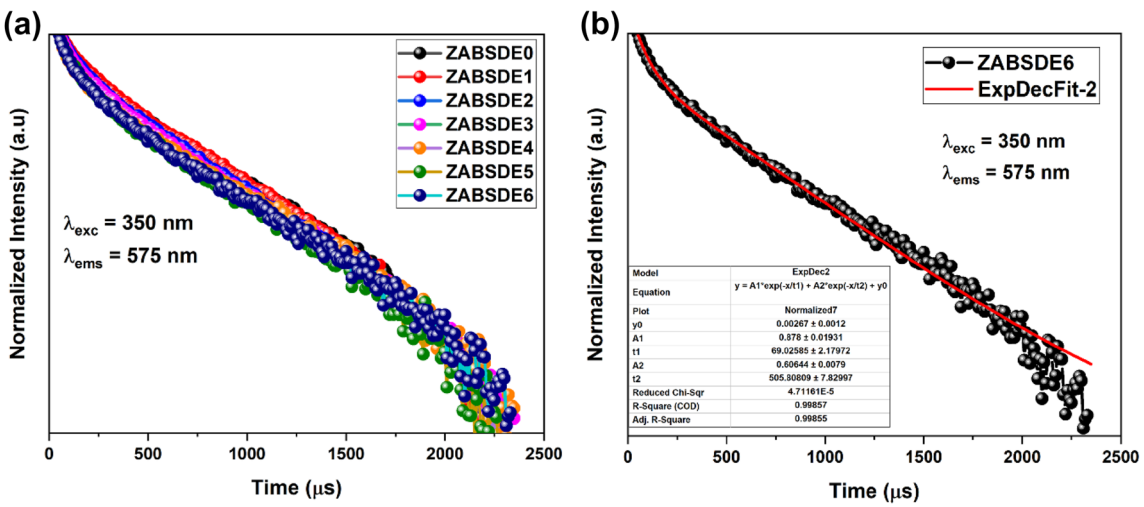

Fig. 7 **a** Decay curves recorded under 350 nm excitation and 575 nm emission, **b** Bi-exponential decay fitting shown for ZABSDE6 glass

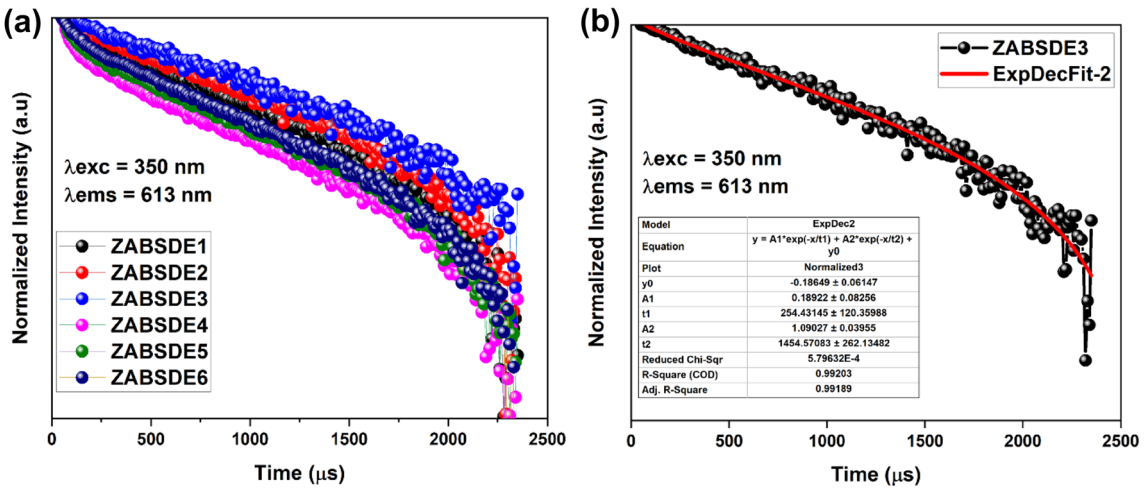

Fig. 8 **a** Decay curves recorded under 350 nm excitation and 613 nm emission, **b** Bi-exponential decay fitting shown for ZABSDE3 glass

Table 2 Experimental lifetimes (τ_{exp}, μs ($\times 10^{-6}s$)), energy transfer parameter (Q), critical energy transfer distance ($R_O \times 10^{-8}cm$), energy transfer efficiency (η_{ET},%), probability of energy transfer ($P_{ET,}s^{-1}$), and donor-acceptor interaction parameter ($C_{DA} \times 10^{-45}cm^6/s$) of Dy^{3+}-Eu^{3+} co-doped ZABS glasses

Glass Code	Dy^{3+} lifetime (τ_{exp})	Eu^{3+} lifetime (τ_{exp})	Q	R_O	η_{ET} (%)	P_{ET}	C_{DA}
ZABSDE0	512.34	–	–	–	–	–	–
ZABDSE1	497.53	905.16	0.2472	1.305	2.890	58.103	9.927
ZABSDE2	481.64	1062.85	0.2941	1.168	5.992	124.41	5.271
ZABSDE3	470.94	1419.21	0.3460	1.079	8.080	171.58	3.350
ZABSDE4	462.18	789.77	0.3943	1.026	9.790	211.83	2.523
ZABSDE5	445.53	773.01	0.4624	1.006	13.040	292.68	2.326
ZABSDE6	433.74	669.68	0.4882	0.964	15.341	353.69	1.850

interactions, respectively. The I-H fitting plot for ZABSDE3 glass is shown in Fig. 9. The best linear fit is seen for $S = 6$, with the R^2 values obtained at 0.99. From the fitting table (inset of Fig. 9) the term Q stands for the energy transfer parameter given as.

$$Q = \frac{4\pi}{3}\Gamma\left(1 - \frac{3}{S}\right)CR_O^3, \tag{7}$$

where C is the concentration of acceptor ions (Eu^{3+}), R_O is the critical energy transfer distance or the distance of a donor-acceptor pair, $\Gamma\left(1 - \frac{3}{S}\right)$ is a constant value which equals to 1.77 for dipole-dipole ($S = 6$), 1.43 for dipole-quadrapole ($S = 8$), and 1.30 for quadrapole-quadrapole ($S = 10$) [22]. From Eq. (7) the R_O value is obtained. Using the $R_O$value the donor-acceptor interaction parameter is calculated as follows,

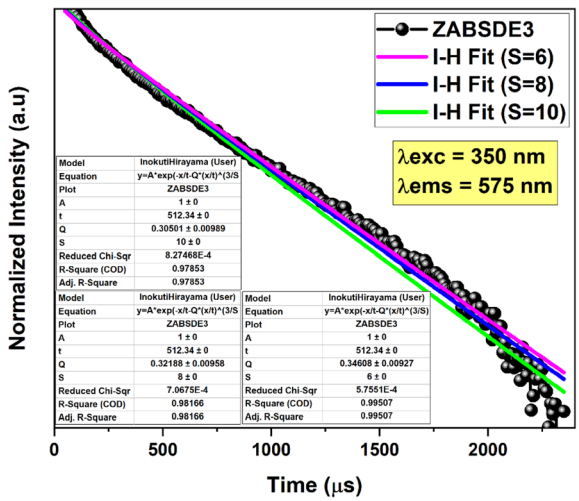

Fig. 9 Inokuti-Hirayama (I-H) fitting plot shown for ZABSDE3 glass

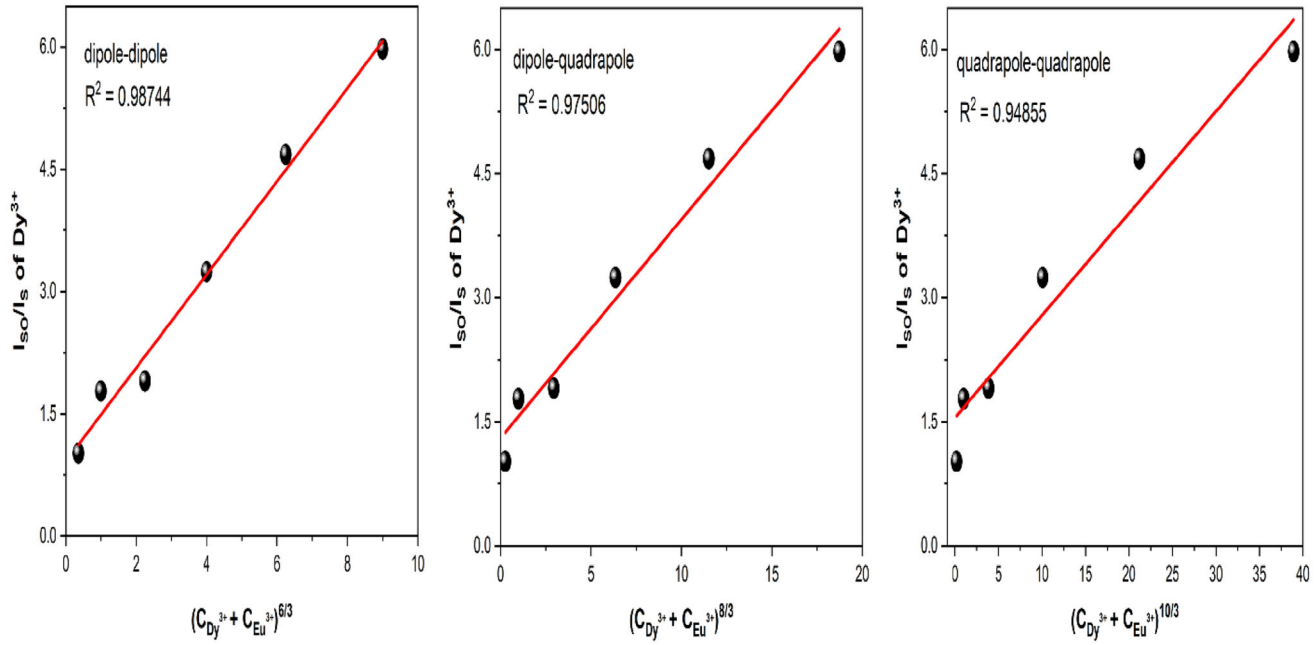

Fig. 10 Dexter energy model showing the dipole-dipole interaction between Dy^{3+} and Eu^{3+} ions

$$C_{DA} = \frac{R_O^S}{\tau_O} \tag{8}$$

The calculated values are grouped in Table 2. The energy transfer (Q), energy transfer efficiency (η_{ET}), and probability of energy transfer (P_{ET}) are all found to increases with increasing Eu^{3+} concentration, while the critical energy transfer distance (R_O), and donor-acceptor interaction parameter (C_{DA}) decreases with increasing Eu^{3+} concentration. Thus, from the I-H fitting, it can be deducted that the type of energy migration between Dy^{3+} and Eu^{3+} is 'dipole-dipole' type when the condition $S = 6$ is satisfied.

3.2.5 *Dexter energy transfer model*

The Dexter energy transfer model is simple, and it is adopted when there is a spectral overlap between energy levels of donor and acceptor. The Dexter energy transfer is associated with the term 'quenching' such that the emission spectra is wholly considered. The Dexter's energy transfer (ET) formula along with Reisfeld's approximation is used to determine the type of energy migration in $Dy^{3+} \rightarrow Eu^{3+}$ using the following relation [23, 24].

$$\frac{\eta_o}{\eta} \propto C^{n/3}, \tag{9}$$

where η_o and η represent the quantum efficiency of the Dy^{3+} in absence and presence of Eu^{3+}, respectively; C denotes the concentration of sensitizer (Dy) and activator (Eu) in mol% and n stands for the type of interaction i.e., n = 6, 8, 10 for dipole-dipole, dipole-quadrapole, and quadrapole-quadrupole. Equation (9) can be related to luminescence intensities given as

$$\frac{I_{SO}}{I_S} \propto C^{n/3} \tag{10}$$

Here, I_{SO} and I_S denote the luminescence intensity of Dy^{3+} without Eu^{3+} and with Eu^{3+}, respectively when the glasses are excited at 350 nm. By plotting $\frac{I_{SO}}{I_S}$ versus $C^{n/3}$, the best linear fit can be determined when n = 6, 8, 10. From Fig. 10, it is seen that the best linear fit is obtained best for n = 6, with R^2 = 0.9874 suggesting the dipole-dipole type of interaction between Dy^{3+} and Eu^{3+}. The latter finding is in accordance with the I-H fitting method.

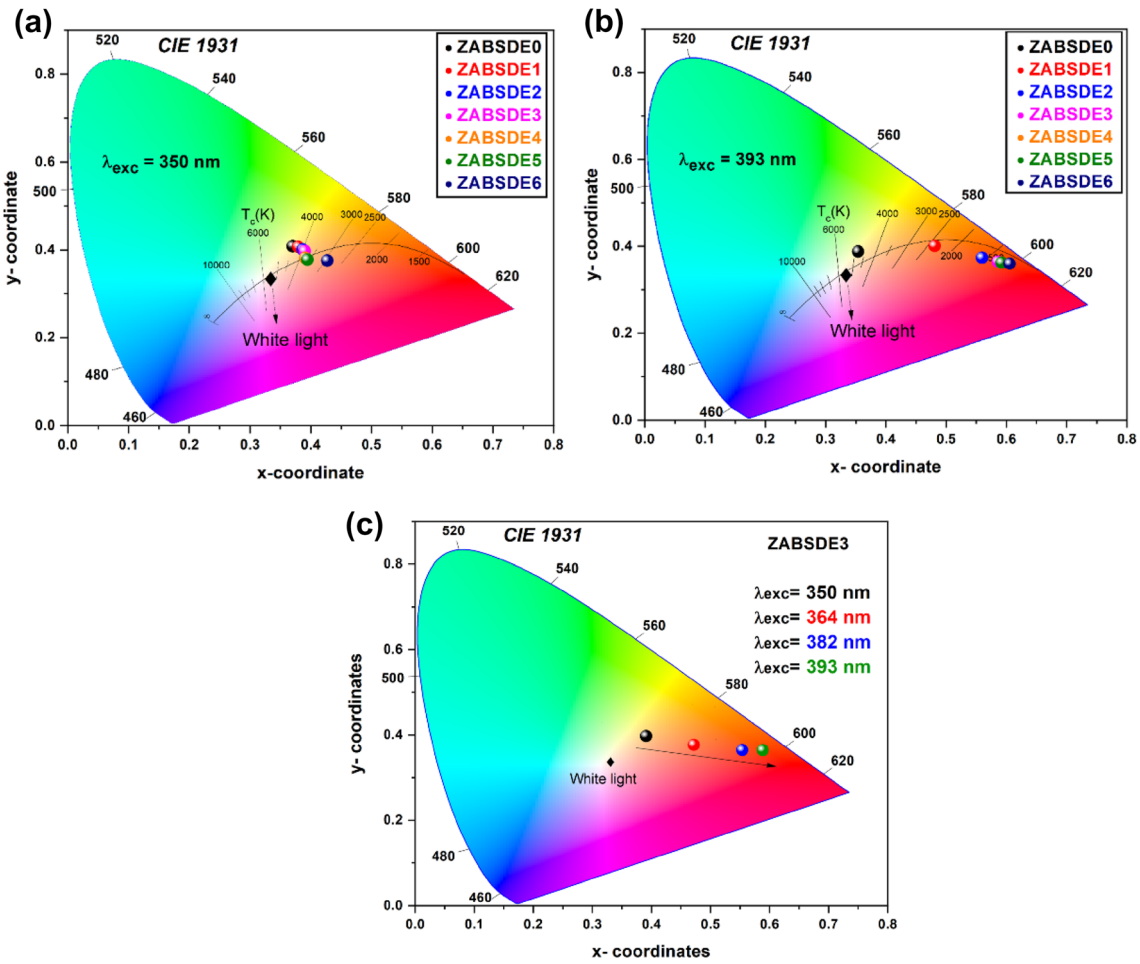

Fig. 11 CIE chromaticity diagrams

Table 3 Evaluated color coordinates (*x*,*y*) and correlated color temperature (CCT, *K*) values for Dy^{3+}-Eu^{3+} co-doped glasses under 350 and 393 nm wavelengths

Glass Code	λ_{exc} = 350 nm			λ_{exc} = 393 nm		
	x	*y*	CCT	*x*	*y*	CCT
ZABSDE0	0.370	0.401	4421	0.353	0.388	4848
ZABSDE1	0.379	0.407	4223	0.480	0.401	2330
ZABSDE2	0.386	0.401	4021	0.559	0.374	1542
ZABSDE3	0.389	0.397	3924	0.585	0.365	1509
ZABSDE4	0.390	0.382	3796	0.588	0.364	1513
ZABSDE5	0.394	0.378	3667	0.591	0.363	1520
ZABSDE6	0.427	0.376	2927	0.605	0.360	1560

3.2.6 *Color coordinates and correlated color temperatures*

The color estimation for the glasses under different excitations were provided by CIE-1931 chromaticity diagram. The CIE plots of glasses under 350 and 393 nm excitations are given in Fig. 11a and Fig. 11b, respectively, and their color coordinates (*x*, *y*) are listed in Table 3. Under 350 nm, the CIE chromaticity coordinates are found to move from a neutral white light (0.370, 0.401) to warm white light (0.427, 0.376) with increased Eu^{3+} content. This change is due to the energy transfer from Dy^{3+} to Eu^{3+}. Moreover, the excitation under 393 nm shifts the coordinates from cool white light to reddish region (0.360, 1560). To know about the color tuneability behaviour of the glasses under different excitation sources, ZABSDE3 glass was selected and excited at different wavelengths at 350 nm, 364 nm, 382 nm, and 393 nm. Under all these excitations, it is noted from Fig. 11c that the color emission from the glass moves from white light region to reddish region. The correlated color temperature (CCT) values were evaluated from the equation given as [25, 26].

$$CCT = (-449n^3 + 3525n^2 - 6823.3n + 5520.33) \quad (11)$$

The variation in CCT values is seen with varying the Eu^{3+} concentration (Table 3). Thus, in the present work, addition of Eu^{3+} ions played a significant role in color emission from neutral white light to warm white light. Therefore, the glasses can be suitable for color tuneable LEDs and near ultra-violet W-LEDs application.

4 Conclusion

Dy^{3+}-Eu^{3+} co-doped glasses were prepared using a high-temperature melt-quenching method. The UV-Visible-NIR study revealed the presence of Dy^{3+} and Eu^{3+} transitions with overlap of Dy-Eu peaks. The bandgap and Urbach energy values followed reverse trend with varying Eu^{3+} ions. Emission studies revealed that Dy^{3+} ions exhibit energy transfer to Eu^{3+} ions through non-radiative process under 350 nm excitation. The dipole-dipole type of interaction between Dy^{3+} and Eu^{3+} is determined using the I-H fitting model and dexter energy model. The chromaticity coordinates obtained for lower concentration of Eu^{3+} is found to be consistent for white light emission compared to higher Eu^{3+} concentration. The co-doped glass showed color tuneability behaviour with different excitations in the near UV to visible region, favorable for near-ultraviolet light emitting diode applications.

Author contribution

MM - Writing Original draft; MIS - Validation, Conceptualization; NM - Lifetime measurements; JA - Writing, Editing and Proof correction; SDK - Writing, Editing & Proof Reading.

Funding

Open access funding provided by Manipal Academy of Higher Education, Manipal. The authors have not disclosed any funding.

Data availability

The datasets generated during and/or analyzed during the current study are available from the corresponding author on reasonable request.

Declarations

Conflict of interest The authors declare that they have no known conflicts of interest.

References

1. S. Dutta, S. Som, S.K. Sharma, Luminescence and photometric characterization of K^+ compensated $CaMoO_4$:Dy^{3+} nanophosphors. Dalton Trans. **42**, 9654–9661 (2013). https://doi.org/10.1039/C3DT50780G
2. S. Xiaojiao Kang, H. Lu, D. Wang, W. Ling, Lu, Tricolor- and White Light-Emitting Ce^{3+}/Tb^{3+}- coactivated $Li_2Ca_4Si_4O_{13}$ phosphor via energy transfer. ACS Omega **3**(12), 16714–16720 (2018). https://doi.org/10.1021/acsomega.8b01952
3. S. Som, P. Mitra, V. Kumar, V. Kumar, J.J. Terblans, H.C. Swart, S.K. Sharma, The energy transfer phenomena and colour tunability in Y_2O_2S:Eu^{3+}/Dy^{3+} micro-fibers for white emission in solid state lighting applications. Dalton Trans. **43**, 9860–9871 (2014). https://doi.org/10.1039/C4DT00349G
4. Y. Sun, F.Y.M. Liao, J. Ma, X. Wang, D. He, W. Gao, J. Knight, Hu. Lili, Visible emission and energy transfer in Tb^{3+}/Dy^{3+} co-doped phosphate glasses. J. Am. Ceram. Soc.

103(12), 6847–6859 (2020). https://doi.org/10.1111/jace.17391

5. V. Rajeswara Rao, L. Lakshmi Devi, C.K. Jayasankar, W. Pecharapa, J. Keawkhao, Shobha Rani Depuru, luminescence and energy transfer studies of Ce^{3+}/Dy^{3+} doped fluorophosphate glasses. J. Lumin. **208**, 89–98 (2019). https://doi.org/10.1016/j.jlumin.2018.11.053
6. Y. Yimeng, H. Huo, H. Zhang, T. Zhao, Q. Wang, X. Zou, C. Su, Preparation and luminescence of Dy^{3+} doped glass-ceramics containing $ZnMoO_4$. J. Non Cryst. Solids **569**, 120990 (2021). https://doi.org/10.1016/j.jnoncrysol.2021.120990
7. B. Fan Liao, W. Shen, Y. Wu, J. Zhang, Hu, A study on the anti-thermal Dy^{3+}/Eu^{3+} co-doped $BaLa_4Si_3O_{13}$ Red Phosphors for White-Light -Emitting Diodes and Optical Thermometry Applications. Ind. Eng. Chem. Res. **60**, 2931–2943 (2021). https://doi.org/10.1021/acs.iecr.0c05996
8. H. Jialiang Niu, W. Ding, Z. Zhou, D. Zhang, X. Bai, Wang, Investigations on energy transfer mechanism and tunable luminescent properties of co-doped $Ca_9La(PO_4)_7$:Dy^{3+},Eu^{3+} phosphors. Appl. Phys. A **126**, 378 (2020). https://doi.org/10.1007/s00339-020-03563-w
9. K. Anilkumar, S. Damodaraiah, S. Babu, V. Reddy Prasad, Y.C. Ratnakaram, Emission spectra and energy transfer studies in Dy^{3+} and Dy^{3+}/Eu^{3+} co-doped potassium fluorophosphate glasses for white light applications. J. Lumin. **205**, 190–196 (2019). https://doi.org/10.1016/j.jlumin.2018.09.007
10. E. Shelby James, *Introduction to Glass Science and Technology* (Royal Society of Chemistry, London, 2015)
11. D. Ruiwang Liu, M. Wang, L. Chen, Y. Liu, F. Zhou, Zeng, Zhongmin Su, luminescence, energy transfer properties of Dy^{3+}/Eu^{3+} coactivated neutral and warm white emissions GSBG glasses. J. Lumin. **237**, 118180 (2021). https://doi.org/10.1016/j.jlumin.2021.118180
12. A.K. Kaushal Jha, M. Vishwakarma, D. Jayasimhadri, K. Haranath, Jang, Multicolor emission and energy transfer dynamics in thermally stable Dy^{3+}/Eu^{3+} co-doped ZPBT glasses for epoxy free w-LEDs application. J. Non Cryst. Solids **553**, 120516 (2021). https://doi.org/10.1016/j.jnoncrysol.2020.120516
13. D.V. Krishna Reddy, T. Sambasiva Rao, S. Taherunnisa, A. Suchocki, Y. Zhydachevskyy, M. Piasecki, M. Rami, Reddy, Tunable white light by varying excitations in yttrium alumino bismuth borosilicate glasses co-doped with Dy^{3+}- Eu^{3+} for cool WLED applications. J. Non Cryst. Solids **513**, 167–182 (2019). https://doi.org/10.1016/j.jnoncrysol.2019.03.011
14. G. Wenli Zhou, X. Wang, L. Zheng, J. Yu, Z. Zhang, S. Qiu, Lian, Tunable colors and applications of Dy^{3+}/Eu^{3+} co-doped CaO-B_2O_3-SiO_2 glasses. J. Am. Ceram. Soc. **102**(10), 5890–5898 (2019). https://doi.org/10.1111/jace.16442
15. Z. Jingxi An, Y. Zhang, ZhiYuan Qiu, Y. Fu, F. Zhou, Zeng, Luminescence properties of borosilicate glass doped with $Ce^{3+}/Dy^{3+}/Eu^{3+}$ under ultraviolet excitation for white LED. J. Non Cryst. Solids **503–504**, 208–213 (2019). https://doi.org/10.1016/j.jnoncrysol.2018.09.050
16. M.K. Nisha Deopa, P.R. Sahu, R. Rani, A.S. Punia, Rao, Realization of warm white light and energy transfer of Dy^{3+}/Eu^{3+} co-doped Li_2O-PbO-Al_2O_3-B_2O_3 glasses for lighting applications. J. Lumin. **222**, 117166 (2020). https://doi.org/10.1016/j.jlumin.2020.117166
17. P. Yu, W. Guo, R. Zhang, L. Su, J. Xu, White and tunable light emission in Eu^{3+}, Dy^{3+} codoped phosphate glass. Opt. Mater. **114**, 110939 (2021). https://doi.org/10.1016/j.optmat.2021.110939
18. J. Tauc, Optical properties and electronic structures of amorphous Ge and Si. Mater. Res. Bullet **3**(1), 37–46 (1968). https://doi.org/10.1016/0025-5408(68)90023-8
19. E.A. Davis, N.F. Mott, Conduction in non-crystalline systems V, Conductivity, optical absorption, and photoconductivity in amorphous semiconductors. Taylor& Francis **22**(179), 0903–0922 (1970). https://doi.org/10.1080/14786437008221061
20. M. Monisha, N. Mazumder, S.K. Melanthota, B. Padasale, H. Aljawhara, M.I. Almuqrin, N. Sayyed, D. Karunakara, Sudha, Kamath, Enhancement of dysprosium oxide doped zinc alumino borosilicate glasses in thermal, optical and luminescence domain for solid state lighting application. Opt. Mater. **128**, 112447 (2022). https://doi.org/10.1016/j.optmat.2022.112447
21. A. Vinod Hegde, H. Wagh, C.S. Hegde, S.D. Dwaraka Vishwanath, Kamath, Spectroscopic investigation on europium doped heavy metal borate glasses for red luminescent applications. Appl. Phys. A **123**, 302 (2017). https://doi.org/10.1007/s00339-017-0914-5
22. M. Vijayakumar, K. Marimuthu, Tailoring the luminescence of Eu^{3+} co-doped Dy^{3+} incorporated aluminofluoroborophosphate glasses for white light applications. J. Lumin. **178**, 414–424 (2016). https://doi.org/10.1016/j.jlumin.2016.06.016
23. F. Bin, W. Zhao, L. Han, Eu^{3+} co-doped $Sr_3Gd(PO_4)_3$:Dy^{3+} phosphors: luminescence properties and color-tunable white-light emission for NUV-WLEDs. Appl. Phys. A **126**, 260 (2020). https://doi.org/10.1007/s00339-020-3444-5
24. G. Li, D. Geng, M. Shang, C. Peng, Z. Cheng, J. Lin, Tunable luminescence of Ce^{3+}/Mn^{2+} -coactivated $Ca_2Gd_8(SiO_4)_6O_2$ through energy transfer and modulation of excitation: poten-

tial single-phase white/yellow-emitting phosphors. J. Mater. Chem. **21**, 13334 (2011). https://doi.org/10.1039/C1JM11650A

25. C.-H. Huang, T.-W. Kuo, T.-M. Chen, Novel red-emitting Phosphor $Ca_9Y(PO_4)7$: Ce^{3+}, Mn^{2+} with energy transfer for fluorescent lamp application. ACS Appl. Mater. Inter. **2**(5), 1395–2010 (2010). https://doi.org/10.1021/am100043q
26. C.S. McCamy, Correlated color temperature as an explicit function of chromaticity coordinates. Color. Res. Appl. **17**, 142–144 (1992). https://doi.org/10.1002/col.5080170211